Sideband separation experiments in NMR with phase incremented echo train acquisition

Brennan J. Walder,[1] Krishna K. Dey,[2] Derrick C. Kaseman,[1] Jay H. Baltisberger,[3] and Philip J. Grandinetti[1,a)]

[1]*Department of Chemistry, Ohio State University, 100 West 18th Avenue, Columbus, Ohio 43210, USA*
[2]*Center of Biomedical Magnetic Resonance, SGPGIMS Campus, Lucknow, India*
[3]*Division of Natural Science, Mathematics, and Nursing, Berea College, Berea, Kentucky 40403, USA*

(Received 27 September 2012; accepted 16 April 2013; published online 7 May 2013)

A general approach for enhancing sensitivity of nuclear magnetic resonance sideband separation experiments, such as Two-Dimensional One Pulse (TOP), Magic-Angle Turning (MAT), and Phase Adjust Spinning Sidebands (PASS) experiments, with phase incremented echo-train acquisition (PIETA) is described. This approach is applicable whenever strong inhomogeneous broadenings dominate the unmodulated frequency resonances, such as in non-crystalline solids or in samples with large residual frequency anisotropy. PIETA provides significant sensitivity enhancements while also eliminating spectral artifacts would normally be present with Carr-Purcell-Meiboom-Gill acquisition. Additionally, an intuitive approach is presented for designing and processing echo train acquisition magnetic resonance experiments on rotating samples. Affine transformations are used to relate the two-dimensional signals acquired in TOP, MAT, and PASS experiments to a common coordinate system. Depending on sequence design and acquisition conditions two significant artifacts can arise from truncated acquisition time and discontinuous damping in the T_2 decay. Here we show that the former artifact can always be eliminated through selection of a suitable affine transformation, and give the conditions in which the latter can be minimized or removed entirely. [http://dx.doi.org/10.1063/1.4803142]

I. INTRODUCTION

When a sample rotates in a magnetic field, its magnetic resonance spectrum splits into a centerband resonance flanked by spinning sidebands at integer multiples of the spinning speed.[1] While spinning sideband resonances are often perceived as a spectral complication to be eliminated, they also contain valuable information about the frequency anisotropy.[2] For example, in solid-state Magic-Angle Spinning (MAS) NMR spectra of spin 1/2 nuclei the rotor-modulated frequency contribution provides information about the 2nd-rank chemical shift frequency anisotropy, whereas the unmodulated frequency contribution is the isotropic (0th-rank) chemical shift. In a similar way the dipolar coupling and nuclear electric field gradient for coupled nuclei and quadrupolar nuclei, respectively, can be measured. In magnetic resonance imaging, a separation of modulated and unmodulated frequency contributions while a sample rotates in a magnetic field gradient can be used to reconstruct a three-dimensional image of the sample within the rotor.[3–5]

Since the seminal work of Dixon,[6] various methods for separating the modulated and unmodulated contributions to a transition frequency in a rotating sample have been proposed. The central idea behind these methods is a recognition that the signal phase contributions from both rotor-modulated and unmodulated frequencies, which are parametrically dependent on the same time variable, can be separated by splitting their evolution into orthogonal time dimensions. Dixon[6] showed in a detailed theoretical analysis that the solution of a set of simultaneous nonlinear equations can provide the timings for a series of π pulses in the Phase Adjust Spinning Sidebands (PASS) experiment for separating the signal phase evolution arising from rotor-modulated and unmodulated frequencies. Unfortunately, the physical picture behind Dixon's discovery was not entirely obvious, and further refinement of his ideas languished for a number of years. Shortly after Dixon, however, Maciel and co-workers[7] developed a related approach called magic-angle hopping (MAH) for separating isotropic and anisotropic contributions of spin 1/2 nuclei. Their approach was physically intuitive as it was based on simple symmetry arguments.[8,9] In subsequent years, a sequence of refinements to MAH dramatically improved its utility. First, Gan[10] realized that hopping could be replaced with slow turning without compromising the separation of isotropic and anisotropic contributions. Next, Grant and co-workers[11] and Pines and co-workers[12] showed that the sensitivity of Gan's magic-angle turning (MAT) experiment could be improved by using π pulses instead of $\pi/2$ pulses to eliminate undesired transverse evolution. During this period, Levitt and co-workers[13] began a detailed analysis of Dixon's approach and showed that both PASS and MAT are solutions to Dixon's equations with different boundary conditions. A thorough review of such solutions are described by Antzutkin.[14] Note that Antzutkin refers to the family of MAT solutions in his review as Isotropic Rotation Sequences (IRS).

The fundamental difference between the π pulse version of MAT and Levitt's version of PASS is that the former has a constant-time-indirect dimension for

a)grandinetti.1@osu.edu

unmodulated (e.g., isotropic) frequency evolution while the latter has a constant-time-indirect dimension for rotor-modulated (e.g., anisotropic) frequency evolution. Because the rotor-modulated frequency evolution is periodic with the rotor period, Levitt and co-workers argued that pure rotor-modulated signal phase evolution is the natural choice for the constant time indirect dimension.[13] This idea was further strengthened by the failure of MAT methods to provide an unmodulated frequency evolution dimension without signal artifacts arising from truncated acquisition and discontinuous signal damping.[15] Thus, PASS appears to be the more robust of the two approaches, although the complicated π pulse timings needed for PASS make it more challenging to implement on older commercial NMR spectrometers.

In previous work,[16] we have shown that the direct and indirect dimensions of a 2D PASS experiment can be interchanged in a signal processing step: a double shear transformation called Two-Dimensional One Pulse (TOP), modeled after the Two-dimensional One-Pulse experiments of Blümich and co-workers.[17,18] The TOP transformation effectively swaps the sampling intervals in the direct dimension and indirect dimensions. This allows the sampling interval in the rotor-modulated evolution dimension of PASS to be taken from the direct dimension, typically allowing a significant reduction in the minimum time required to perform a PASS experiment. Here we show that the TOP transformation can also be applied to a MAT signal to eliminate its truncated acquisition artifact. A similar idea, first described by Levitt and co-workers[13] and later by Gan and co-workers,[19,20] is to use shifting acquisition periods instead of a post-acquisition signal transformation.

We also demonstrate here how echo train acquisition can be appended to either PASS or MAT with equal gains in sensitivity. In contrast to recent claims[20] that echo train acquisition cannot be appended to PASS with the same sensitivity gain as MAT, here we show that a solution comes in realizing that the train of echo-refocusing π pulses must be equally spaced and positioned at times where the sum of the indirect and direct rotor modulated evolution phase is an integer multiple of 2π.

Finally, because both PASS and MAT have phase modulated signals before detection, the conventional echo train acquisition approach of Carr-Purcell-Meiboom-Gill (CPMG) can result in signal artifacts from undesired coherence transfer pathways unless a z filter or complicated phase cycle with multiplex acquisition is implemented.[20] Here we present a simpler approach based on the recently introduced "Phase Incremented Echo Train Acquisition" (PIETA) technique,[21] which eliminates the need for a z filter or such multiplex acquisition schemes. PIETA, unlike CPMG, also creates opportunities to turn echo train acquisition in J-coupled spin systems into a J-resolved dimension.[21]

II. EXPERIMENTAL

Approximately 2 g of $KMg_{0.5}O \cdot 4SiO_2$ glass was synthesized from K_2CO_3 (Aldrich, 99+%), MgO (Alfa Aesar, 99.95%), SiO_2 (Aldrich, 99.995%), and CuO (Mallinckrodt). Prior to synthesis, the K_2CO_3 and MgO were placed in a dehydrating furnace at 150 °C overnight to remove any water from the sample. The starting materials were ground and placed in a furnace at 600 °C overnight to decarbonate followed by melting at 1400 °C for 1.5 h. Each sample was quenched by placing the bottom of the platinum crucible in water. Each sample was ground into a powder and packed in a rotor in a nitrogen filled glove bag.

All NMR experiments were performed on a Bruker Avance operating at a field strength of 9.4 tesla, utilizing spectrometer frequencies of 100.737 MHz for ^{13}C, 400.586 MHz for ^{1}H, 79.578 MHz for ^{29}Si, and 131.072 MHz for ^{87}Rb. All four-dimensional PIETA signals were reduced down to two dimensions, eliminating the PIETA phase and echo count dimensions as described elsewhere.[21] After TOP processing, four repeats of the acquired 2D signal in the periodic modulated evolution dimension was performed to separate sidebands. Signal-to-noise calculations, however, were based on spectra processed with no signal repeats to avoid an artificial boost of the sensitivity.

The MAT pulse sequence shown in Fig. 1 was performed on L-Histidine monochloride monohydrate (Sigma Aldrich) using a commercial Bruker 7 mm double resonance MAS probe with a rotor frequency of 1250 ± 2 Hz. The indirect dimension was incremented from $-t_R/2$ to $t_R/2$ in 32 steps.

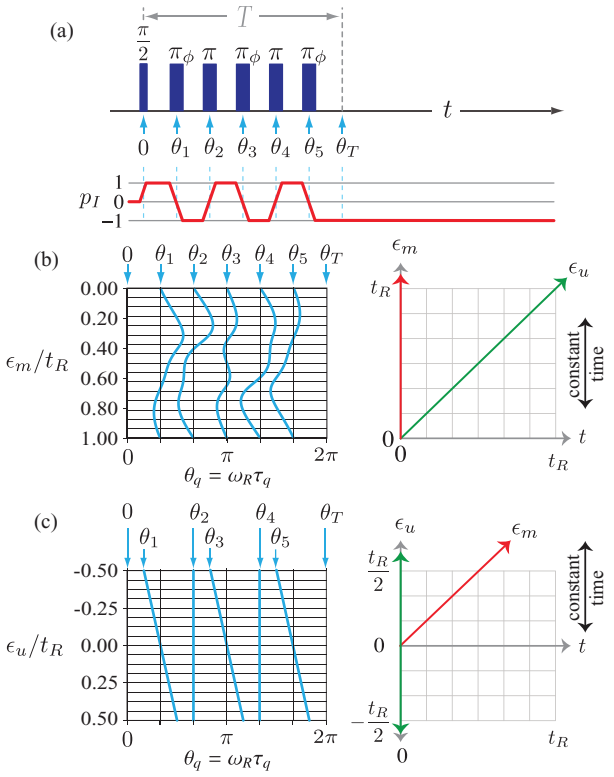

FIG. 1. (a) A generic five π pulse sequence when $L_{max} = 2$ for both the PASS and MAT experiments along with p_I symmetry pathway.[9] The θ_j represent the rotor position $\theta_j = \omega_R t_j$ where t_j is the time from the initial excitation pulse. Instead of traditional phase cycling, the signal is acquired with a constant receiver phase while the phase of all π pulses with the ϕ subscript are incremented together into a single phase dimension.[21] (b) The π pulse timings for the PASS experiment along with symmetry pathways and the lines in the ϵ_m-t coordinates where the unmodulated and modulated evolutions refocus into echoes. (c) The π pulse timings for the MAT experiment along with symmetry pathways and the lines in the ϵ_u–t coordinates where the unmodulated and modulated evolutions refocus into echoes. In both (b) and (c) the direction of constant time relative to the initial excitation pulse is indicated.

The phase dimension was incremented in steps of $2\pi/16$. The rf field strength of ^{1}H were 20 kHz and 35 kHz for initial excitation and two-pulse phase-modulated (TPPM) decoupling, respectively. The rf field strength during ^{1}H-^{13}C cross-polarization was 19.2 kHz and the contact time of 0.6 ms was used. Twenty four scans per phase slice were collected at a recycle delay of 6 s. The total experiment time was 20 h 32 min.

The MAT-PIETA pulse sequence, shown in Fig. 5, was performed on a sample of Cu(II) doped $KMg_{0.5}O \cdot 4SiO_2$ glass using a commercial Bruker 7 mm double resonance MAS probe with a rotor frequency of 790 ± 1 Hz. The indirect dimension was incremented from $-t_R/2$ to $t_R/2$ in 32 steps. The phase dimension was incremented in steps of $2\pi/128$. The rf field strength for all pulses on ^{29}Si was 50.8 kHz. The recycle delay used was 20 s, with one scan per PIETA phase increment. The total experiment time was 23 h 6 min.

The shifted-echo QMAT and QMAT-PIETA pulse sequences applied to polycrystalline Rb_2SO_4 (Aldrich) were identical those shown in Fig. 5, except the five π pulse preparation was replaced with a nine π pulse preparation described elsewhere.[22,23] Experiments were performed in a Bruker 4 mm MAS probe spinning at 2604 ± 1 Hz. A rf field strength of 30 kHz was used for selective excitation of the central transition. The indirect dimension was incremented from $-t_R/2$ to $t_R/2$ in 32 steps. The phase dimension was incremented in steps of $2\pi/64$. Twelve scans per PIETA phase increment were collected at a recycle delay of 0.75 s. The total experiment time was 5 h 55 min.

III. RESULTS AND DISCUSSION

A. Background

The NMR transition frequency becomes time dependent during sample rotation. A multipole expansion of this frequency can be separated into rotor-modulated and unmodulated components:

$$\Omega(\phi_R) = \sum_{l=0}^{L_{\max}} \omega_{l,0} + \sum_{l=1}^{L_{\max}} \sum_{\substack{k=-l \\ k\neq 0}}^{l} \omega_{l,k} e^{ik\phi_R}, \tag{1}$$

where ϕ_R is the rotor phase and $L_{\max}$ is the highest rank anisotropy contributing to the NMR frequency. The rotor phase advances under sample rotation according to

$$\phi_R = \omega_R t + \chi_R, \tag{2}$$

where ω_R is the rotor frequency, t is the duration of rotation, and χ_R is the initial rotor phase.

After an excitation pulse, the phase of the NMR signal for a rotating sample is given by

$$\Phi(t) = \int_0^t \Omega(\omega_R t' + \chi_R)\, dt', \tag{3}$$

where t is the signal evolution time after the pulse. Substituting Eq. (1) into Eq. (3) one obtains

$$\Phi(t) = W_0 t + \sum_{l=1}^{L_{\max}} \sum_{\substack{k=-l \\ k\neq 0}}^{l} W_{l,k}(\chi_R)[e^{ik\omega_R t} - 1], \tag{4}$$

where we have defined

$$W_0 = \sum_{l=0}^{L_{\max}} \omega_{l,0} \quad \text{and} \quad W_{l,k}(\chi_R) = \frac{\omega_{l,k}}{ik\omega_R} e^{ik\chi_R}.$$

We can visualize the one-dimensional signal phase of Eq. (4) as a cross section along the line $t = t_u = t_m$ through a two-dimensional signal in a t_u–t_m coordinate system where the phase of this 2D signal would be given by

$$\Phi(t_m, t_u) = W_0 t_u + \sum_{l=1}^{L_{\max}} \sum_{\substack{k=-l \\ k\neq 0}}^{l} W_{l,k}(\chi_R)[e^{ik\omega_R t_m} - 1]. \tag{5}$$

An important feature of this 2D signal is that it is periodic along the t_m dimension according to

$$\Phi(t_m + nt_R, t_u) = \Phi(t_m, t_u), \tag{6}$$

where n is an integer.

The significance of the t_u–t_m coordinate system is that only the rotor-modulated frequency contributions evolve along the t_m dimension while only unmodulated frequency contributions evolve along the t_u dimension. It was Dixon[6] who first showed that the full two-dimensional signal phase in Eq. (5) can be obtained for arbitrary values of t_u and t_m by applying a series of π pulses carefully timed relative to the rotor phase after the excitation pulse. As described in the supplementary material,[51] the timings for the π pulses are obtained from the simultaneous solution of a set of nonlinear equations.[6]

The signal phase in a PASS or MAT experiment is not measured along orthogonal dimensions of t_u and t_m, but rather in a 2D ϵ–t coordinate system that is related to the desired t_u–t_m coordinate system by an affine transformation.[16] Both PASS and MAT can be implemented with five π pulses when $L_{\max} = 2$ with a sequence illustrated in Fig. 1(a). While PASS and MAT solutions employing other than five π pulses exist,[14] we consider only the five π pulse solutions without any loss of generality. We also only consider π pulses occurring inside a constant time period T, which is an integer number of rotor periods (typically one rotor period), as shown in in Fig. 1(a).

In the PASS experiment, the timings of the π pulses are chosen so that at $t = 0$ the signal phase has the form

$$\Phi_{\text{PASS}}(\epsilon_m, 0) = -\sum_{l=1}^{L_{\max}} \sum_{\substack{k=-l \\ k\neq 0}}^{l} W_{l,k}(\chi_R)[e^{ik\omega_R \epsilon_m} - 1]. \tag{7}$$

Notice that the PASS signal is designed so there is no unmodulated evolution phase during ϵ_m and that the rotor-modulated evolution phase goes "backward" during ϵ_m and "forward" during t leading to the refocusing of the rotor-modulated evolution into an echo during t along the line $t - \epsilon_m = 0$. The acquired PASS signal, like Eq. (6), also has translational symmetry given by

$$\Phi_{\text{PASS}}(\epsilon_m + nt_R, t) = \Phi_{\text{PASS}}(\epsilon_m, t), \tag{8}$$

where n is an integer.

In the MAT experiment, the timings of the π pulses are chosen so that at $t = 0$, the signal phase has the form

$$\Phi_{\text{MAT}}(\epsilon_u, 0) = -W_0 \epsilon_u. \tag{9}$$

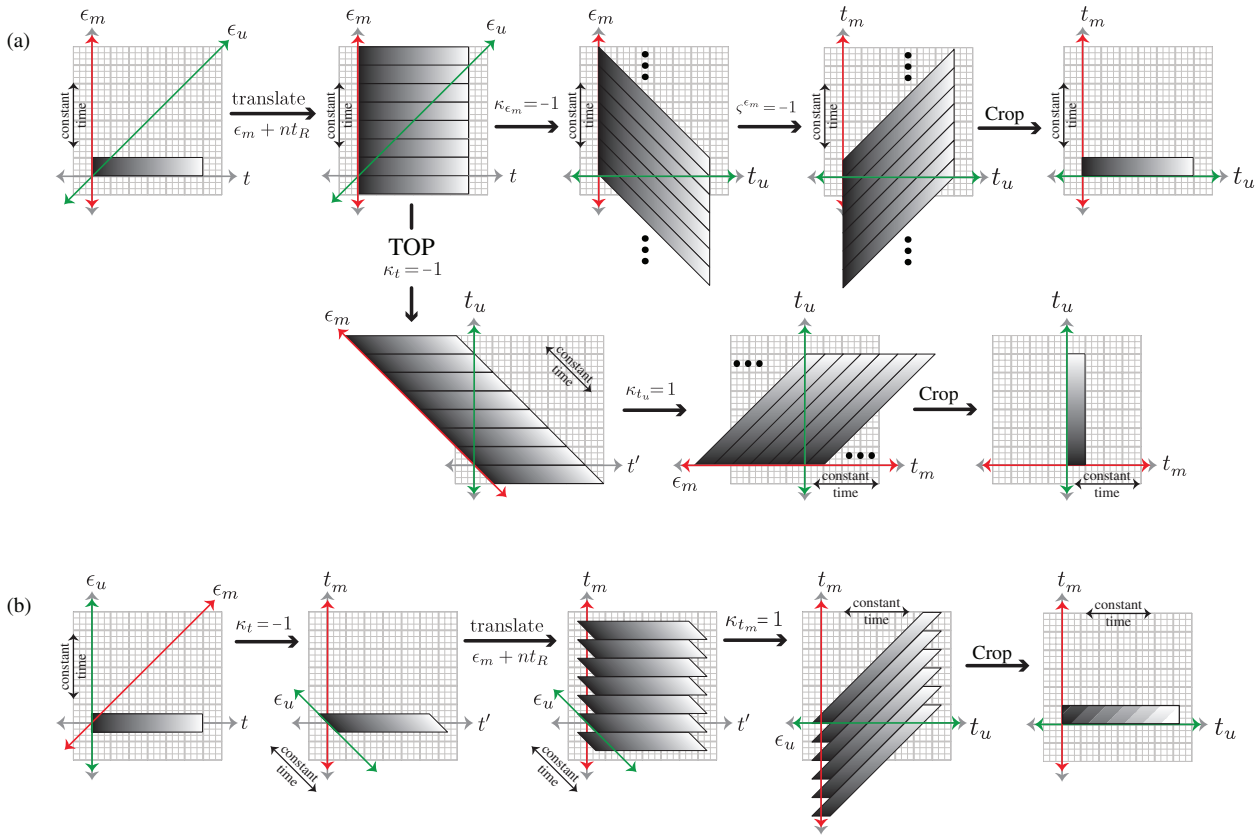

FIG. 2. Transformation of acquired signals, shown as grayscale-filled rectangle, into a 2D signal that correlates rotor-modulated evolution to unmodulated evolution. The gray scale gradient represents the signal envelope decay due to T_2 processes. The symbol ϵ_u labels the line along which pure unmodulated evolution occurs (green), while the symbol ϵ_m labels the line along which pure rotor-modulated evolution occurs (red). Along the direct acquisition dimension, t, both rotor-modulated and unmodulated evolution occur. The direction of lines of constant time from the initial excitation pulse of the sequence are also indicated. (a) Acquired PASS signal: In the first step, copies of acquired signal are translated according to Eq. (8). Moving from left to right above is the conventional PASS transformation consisting of a single shear parallel to the ϵ_m axis and sheared towards negative values of ϵ_m followed by a negative scaling along the ϵ_m dimension. Moving from left to right below is the TOP-PASS transformation consisting of a first shear that is parallel to the t dimension and sheared towards negative values of t. This shear is followed by a second shear parallel to the t_u dimension and sheared towards positive values of t_u. At the end of the conventional and TOP processing paths the desired digital signal is obtained by cropping out a 2D signal from one or more rotor periods of evolution along the t_m dimension. The advantage of applying the TOP transformation to a PASS signal is that it can significantly reduce the number of samples required in the indirect dimension. (b) Acquired MAT signal: The affine transformation begins with a negative shear, $\boldsymbol{K}_t$, parallel to t, to create a 2D signal with unmodulated frequencies refocused along the vertical axis and the modulated frequencies refocused along $t' + t_m = 0$. At this stage, the signal is "PASS"-like and copies of the signal can be translated according to Eq. (8). Then a positive shear, $\boldsymbol{K}_{t_m}$, parallel to the vertical axis, t_m. At the end of the processing paths the desired digital signal is obtained by cropping out a 2D signal from one or more rotor periods of evolution along the t_m dimension.

The timings of the π pulses for the MAT experiment are designed so there is no rotor-modulated evolution phase during ϵ_u and the unmodulated evolution phase evolves "backward" during ϵ_u and "forward" during t leading to a refocusing of the unmodulated evolution into an echo during t along the line $t - \epsilon_u = 0$.

Instead of traditional pulse phase cycling,[24,25] the MAT or PASS signal can be acquired with a constant receiver phase while the phase of all π pulses having the ϕ subscripts shown in Fig. 1 are incremented together into a single phase dimension.[21] This results in a three-dimensional signal that is a function of ϵ, t, and ϕ. A Fourier transform of the 3D signal with respect to this pulse phase dimension yields the "accumulated" Δp spectrum from which the cross section at $\Delta p = -6$ contains the desired 2D MAT or PASS signal.

Both the MAT and PASS sequence of pulses can be modified for shifted-echo acquisition[26–28] by inserting n rotor periods before one of the preparatory π pulses as shown in the supplementary material.[51] In shifted-echo acquisition the time origin is shifted into the acquisition window by nt_R. Shifted-echo acquisition can be advantageous, particularly for non-crystalline samples, where there is a strongly inhomogeneous broadening of resonances in the direct dimension.

B. PASS, TOP-PASS, and TOP-MAT

The main advantage of PASS over MAT is that the signal in the indirect dimension, ϵ_m, is periodic with the rotor phase. For this reason, the PASS experiment only needs to sample the indirect dimension over a single rotor period. This is illustrated in the coordinate system at the far left of Fig. 2(a). Here the grayscale rectangle represents the 2D PASS signal sampled over one rotor period in ϵ_m, and the grayscale transition from black to white represents the natural T_2 decay of the signal envelope. The symbol ϵ_u labels the line along which pure unmodulated evolution occurs, while the symbol ϵ_m labels the line along which pure rotor-modulated

evolution occurs. Along the direct acquisition dimension, t, both rotor-modulated and unmodulated evolution occur. The direction of lines of constant time from the initial excitation pulse of the sequence are also indicated in this figure. An affine transformation can be applied to this signal to separate the pure rotor-modulated and unmodulated evolutions into orthogonal dimensions. One way to view the affine transformation of the 2D PASS signal is to imagine the digital sampling along the ϵ_m dimension as extending from $-\infty$ to $+\infty$. This can be achieved by translating copies of the acquired signal according to Eq. (8), as illustrated after the first step of Fig. 2(a). From here the transformation can take one of two paths. Moving to the right is the conventional PASS transformation consisting of a single shear parallel to the ϵ_m axis and sheared towards negative values of ϵ_m, specified with a shear constant, $\kappa_{\epsilon_m} = -1$ followed by a scaling along the ϵ_m dimension with a scaling constant $\varsigma^{\epsilon_m} = -1$ according to

$$\begin{bmatrix} t_m \\ t_u \end{bmatrix} = \underbrace{\begin{bmatrix} -1 & 0 \\ 0 & 1 \end{bmatrix}}_{\boldsymbol{S}_{\epsilon_m}} \underbrace{\begin{bmatrix} 1 & -1 \\ 0 & 1 \end{bmatrix}}_{\boldsymbol{K}_{\epsilon_m}} \begin{bmatrix} \epsilon_m \\ t \end{bmatrix}, \\ = \begin{bmatrix} -1 & 1 \\ 0 & 1 \end{bmatrix} \begin{bmatrix} \epsilon_m \\ t \end{bmatrix}. \tag{10}$$

After this transformation the desired digital signal in the desired t_u–t_m coordinate system can be obtained by cropping out a 2D signal from one or more rotor periods of evolution along the ϵ_m dimension. Notice that the grayscale transition of the cropped 2D signal remains continuous and identical to the originally acquired signal.

In practice, the acquired signal in conventional PASS processing is repeated only two or four times along the ϵ_m coordinate without any cropping of the final signal. While this signal repeat is not required it is done to give the appearance of separated spinning sidebands after the discrete Fourier transform. When actively shearing a discretely sampled 2D signal it is convenient to exploit the Fourier affine theorem,[9,29] where the affine transformation is implemented in the inverse domain. A convenient consequence of this approach is that signal sheared outside the acquisition period is aliased back. As long as the acquisition period is an integer multiple of the rotor period, however, this aliasing has no consequence since it results in signal translation commensurate with the symmetry of Eq. (8).

In the context of NMR spectroscopy, Eq. (6) requires that additional care be taken when applying the discrete Fourier transform to the signal along the t_m dimension. An underlying assumption behind the discrete Fourier transform is that the signal is periodic for all time with a period equal to the acquisition time. For a signal sampled for a full rotor period along t_m this is indeed a correct assumption. For the majority of NMR signals, which are aperiodic, this is not the case, and it is well known that the application of the discrete Fourier transform to an aperiodic signal introduces a baseline offset artifact. For this reason Otting *et al.*[30] introduced the procedure of dividing the amplitude of first point of the NMR signal by 2 to eliminate the baseline artifact which was the source of t_1 ridges in the early days of 2D NMR spectroscopy. Today, many NMR processing programs automatically perform this divide by 2 correction before applying a discrete Fourier transform. However, if this correction is mistakenly applied to a truly periodic signal, such as the signal along t_m, then a baseline roll artifact will be introduced into the spectrum. Thus, special care must be taken to set the appropriate software flag so this correction is not performed when Fourier transforming along the t_m coordinate, while retaining this correction when Fourier transforming along the t_u coordinate.

Recently, Davis *et al.*[16] introduced the TOP-PASS approach where the same double shear transformation as used in the TOP experiment[17,31] is applied to the PASS signal to give the t_u dimension the sampling interval of the ϵ_m dimension and the t_m dimension the sampling interval of the t dimension. This approach can significantly reduce the number of acquisition steps required in the indirect dimension, ϵ_m. The TOP processing path, labeled in Fig 2(a), consists of two shears. The first shear is parallel to the t dimension and sheared towards negative values of t, specified with a shear constant, $\kappa_t = -1$. This shear is followed by a second shear parallel to the t_u dimension and sheared towards positive values of t_u, specified with a shear constant, $\kappa_{t_u} = 1$, according to[32]

$$\begin{bmatrix} t_u \\ t_m \end{bmatrix} = \underbrace{\begin{bmatrix} 1 & 1 \\ 0 & 1 \end{bmatrix}}_{\boldsymbol{K}_{t_u}} \underbrace{\begin{bmatrix} 1 & 0 \\ -1 & 1 \end{bmatrix}}_{\boldsymbol{K}_{t}} \begin{bmatrix} \epsilon_m \\ t \end{bmatrix}, \\ = \begin{bmatrix} 0 & 1 \\ -1 & 1 \end{bmatrix} \begin{bmatrix} \epsilon_m \\ t \end{bmatrix}. \tag{11}$$

After the TOP affine transformation, the desired digital signal can be obtained by cropping out a 2D signal from an integer number of rotor periods along the t_m dimension. Again, notice that the grayscale transition of the cropped 2D signal remains continuous and identical to the originally acquired signal.

In practice, the TOP processing of a PASS signal requires numerous signal repetitions along the indirect coordinate, ϵ_m, in order to prevent truncation of the signal along the t_u coordinate in the final transformed signal. Because the dwell time of direct coordinate, t becomes associated with t_m after the TOP processing, care must also be taken to set the direct dimension dwell time to an integer divisor of the rotor period, otherwise interpolation may be required to crop out an integer number of rotor periods along the t_m dimension. Alternatively, instead of cropping, a gaussian apodization applied along the t_m dimension will also give the appearance of separated spinning sidebands after the Fourier transform.[16] The only difference is that the spinning sidebands will appear as gaussian lineshapes instead of lines.

A disadvantage of MAT is that the indirect dimension, ϵ_u, needs to be sampled with an acquisition length that does not truncate the unmodulated evolution of the signal. This can be problematic since the indirect dimension in MAT is a constant time dimension.[15] Here we show that this problem can be overcome by applying the TOP processing approach of Davis *et al.*[16] The MAT signal can be sampled over an indirect acquisition period from $-t_R/2$ to $t_R/2$, and then an affine transformation, as illustrated in Fig. 2(b), is applied to separate the unmodulated and modulated frequency evolution into

orthogonal dimensions. For the MAT signal this can be performed as a double shear, starting with a shear parallel to the t coordinate with a shear ratio of $\kappa_t = -1$, followed by a shear parallel to the t_m coordinate with a shear ratio of $\kappa_{t_m} = 1$, according to

$$\begin{bmatrix} t_m \\ t_u \end{bmatrix} = \underbrace{\begin{bmatrix} 1 & 1 \\ 0 & 1 \end{bmatrix}}_{\boldsymbol{K}_{t_m}} \underbrace{\begin{bmatrix} 1 & 0 \\ -1 & 1 \end{bmatrix}}_{\boldsymbol{K}_t} \begin{bmatrix} \epsilon_u \\ t \end{bmatrix}, \\ = \begin{bmatrix} 0 & 1 \\ -1 & 1 \end{bmatrix} \begin{bmatrix} \epsilon_u \\ t \end{bmatrix}. \quad (12)$$

If desired, the signal can be repeated two or four times along the t_m coordinate after the first shear to give the appearance of separated spinning sidebands after the discrete Fourier transform. After the affine transformation above the acquisition length along the unmodulated evolution, t_u, becomes that of the direct dimension, t. As long as the indirect acquisition period, ϵ_u, is an integer multiple of the rotor period then shearing through the Fourier affine theorem[9,29] will cause signal sheared outside the acquisition period to alias in a manner that is equivalent to a translation having the symmetry of Eq. (6).

In contrast to PASS, where the use of TOP processing is optional, TOP processing is required to eliminate the acquisition truncation artifact in nearly all MAT experiments, the exceptions being samples where significant inhomogeneous broadenings act to dephase the signal completely during the constant time unmodulated evolution period. All further discussions of MAT will assume an indirect dimension sampled from $-t_R/2$ to $t_R/2$ followed by TOP processing.

As before, the desired digitized MAT signal can be obtained by cropping out a 2D signal from one or more rotor periods of evolution along the t_m dimension. Unfortunately, as illustrated in Fig. 2(b) by the grayscale transition, the envelope of the cropped 2D signal contains a discontinuous T_2 dampening. These periodic discontinuities lead to artifacts in the unmodulated dimension that can become significant when T_2 is not significantly greater than the rotor period. While the TOP processing eliminates the artifacts from truncated acquisition times, it introduces artifacts from the discontinuous T_2 dampening. This is a consequence of the lines of constant time from the initial excitation pulse not being parallel to the lines of pure rotor-modulated evolution. This artifact is also present in the recently introduced MAT-PASS experiment of Hung and Gan.[19] That experiment, also described and dismissed by Levitt and co-workers,[13] is essentially identical to TOP-MAT except that the first shear of the TOP transformation is performed through delayed acquisition in t by ϵ_u. This discontinuous dampening artifact in the MAT experiment is not present in PASS experiments, making PASS the preferred approach for separating rotor-modulated and unmodulated evolution. In practice, however, whenever T_2 is significantly longer than a rotor period the discontinuous decay artifacts in MAT will be negligible.

An experimental example of a 2D ^{13}C shielding correlation NMR spectrum of L-Histidine using the TOP-MAT approach is shown in Fig. 3. This spectrum appears identical to the TOP-PASS spectrum of Davis *et al.*[16] This also confirms that MAT or PASS, when combined with TOP processing, can be used to generate the indirect dimension with a minimum sampling. The modulated (sideband) cross sections along with best fit simulations are shown in Fig. 4. Each sideband pattern was fit using a C program employing the polycrystalline integration algorithm based on Lebedev quadrature over the unit sphere, as described by Eden and Levitt.[34]

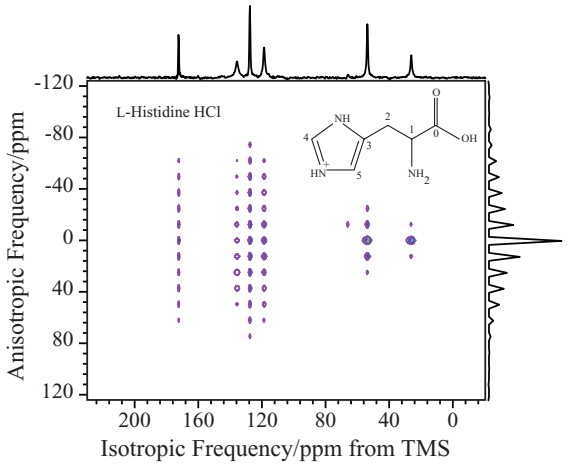

FIG. 3. Two-dimensional MAT spectrum of L-Histidine along with one-dimensional projections. The 2D spectrum was obtained using double shear (TOP) processing.[16] Isotropic frequencies are referenced to Tetramethylsilane (TMS). Contour levels are plotted from 5% to 100% in increments of 5% of the maximum intensity.

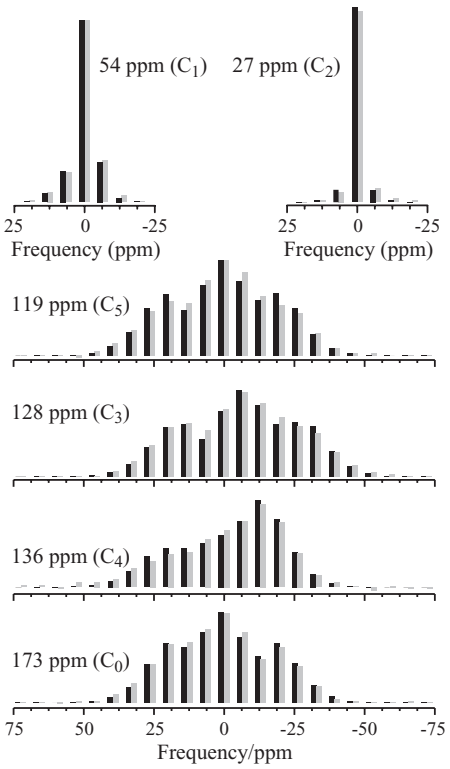

FIG. 4. Rotor modulated cross sections of the L-Histidine TOP-MAT spectrum shown in Fig. 3 along with best-fit simulations for each site. Experimental sideband amplitudes are shown as gray bars while best fit simulations are shown as black bars.

TABLE I. Best fit values of the isotropic shift and principal components of the chemical shift tensor for L-Histidine. All uncertainties are one standard deviation. Also shown, for comparison, are the values obtained by Strohmeier *et al.*[33]

		δ_{xx} (ppm)		δ_{yy} (ppm)		δ_{zz} (ppm)	
Site	δ_{iso} (ppm)	This work	Ref. 33	This work	Ref. 33	This work	Ref. 33
C_0	173.0 ± 2.0	171.3 ± 1.8	...	107.7 ± 1.8	...	239.8 ± 1.8	...
C_1	54.0 ± 2.0	57.8 ± 3.8	57.0	69.1 ± 2.1	68.5	35.1 ± 2.6	37.8
C_2	27.0 ± 2.0	26.8 ± 4.0	...	37.3 ± 2.8	...	16.8 ± 2.2	...
C_3	127.0 ± 2.0	200.3 ± 2.1	198.2	131.6 ± 2.4	132.3	52.0 ± 1.8	49.8
C_4	136.0 ± 2.0	157.8 ± 3.8	...	196.9 ± 3.4	...	53.3 ± 3.4	...
C_5	119.0 ± 2.0	121.0 ± 2.6	122.8	187.5 ± 3.0	190.4	48.4 ± 2.8	44.3

While anisotropic NMR lineshape analyses are often done in a nonlinear least-square approach using the Levenberg-Marquardt algorithm,[35] we have found that a modified boot-strap approach[35] employing a simplex algorithm gives more realistic parameter uncertainties. In the boot-strap approach, the multi-dimensional statistical distribution of model parameters (intensity, δ_{xx}, and δ_{yy}) for each modulated cross section is obtained after multiple least-squares analyses of sideband spectra generated by randomly choosing 32 sidebands with replacement from the experimental 32 sideband spectrum.[35] The mean model parameters with uncertainties using this approach are given in Table I along with previously reported values by Strohmeier *et al.*[33]

C. TOP-MAT and PASS with echo train acquisition

Echo train acquisition (ETA) can be appended to both TOP-MAT and PASS by using the shifted-echo sequence as a starting point. All acquired echoes will be valid MAT or PASS echoes *provided the train of echo-refocusing π pulses*, shown as open rectangles in Fig. 5, *are equally spaced and positioned at times where the sum of the indirect and direct*

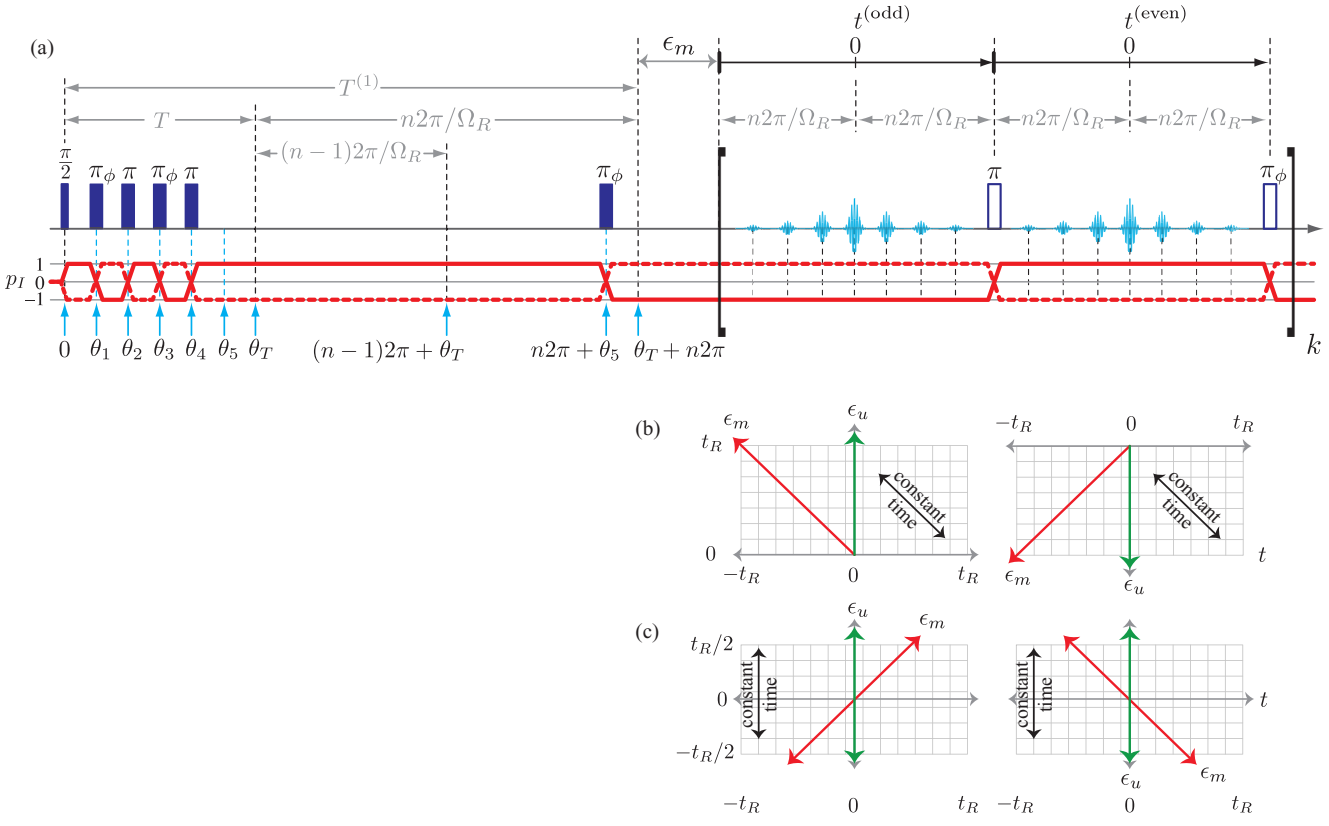

FIG. 5. (a) Five π pulse sequence for TOP-PASS or TOP-MAT with PIETA along with p_I symmetry pathways. Instead of traditional phase cycling, the signal is acquired with a constant receiver phase while the phase of all π pulses with the ϕ subscript are incremented together into a PIETA phase dimension.[21] The θ_j values represent the rotor position $\theta_j = \omega_R t_j$ where t_j is the time from the initial excitation pulse. The PIETA π pulses, shown as unfilled rectangles, must be shifted forward by ϵ_m. In PASS, the values of ϵ_m depend on the timings of the initial five π pulses as illustrated in Fig. 1. In TOP-MAT the value of $\epsilon_m = 0$ for all timings of the initial five π pulses, that is, all echo train acquisition pulses remain at a fixed time from the initial excitation pulse. (b) The lines where the unmodulated and modulated interactions refocus in the ϵ_u-t coordinates for even and odd echoes in the PASS experiment. (c) The lines where the unmodulated and modulated interactions refocus in the ϵ_u–t coordinates for even and odd echoes in the MAT experiment.

rotor modulated evolution phase is an integer multiple of 2π. This is achieved by inserting a delay of ϵ_m before the echo train acquisition, as shown in Fig. 5.

In the case of TOP-MAT, where only unmodulated frequency evolution occurs in the indirect dimension, i.e., $\epsilon_m = 0$, the train of echo-refocusing π pulse positions remain constant relative to the first excitation pulse, i.e., not shifting with changing ϵ_u. This set of timings matches the MAT-CPMG sequence described by Hung *et al.*[20] As shown in Fig. 5(c), the rotor-modulated frequency evolution refocuses into an echo in the middle of each direct dimension of the echo train along the ϵ_u coordinate. The unmodulated frequency evolution refocuses along the line $t^{(\mathrm{odd})} - \epsilon_u = 0$ in odd echoes and along the line $t^{(\mathrm{even})} + \epsilon_u = 0$ in even echoes of the train. While the odd echoes are processed in the same double shearing transformation shown in Fig. 2(b), the even echoes must be processed with opposite signs for the two shearing factors using the double shearing transformation shown in Fig. 2(b) along with a scaling along ϵ_m given by $\varsigma^{\epsilon_m} = -1$. Both even and odd echoes can then be combined in a matched filter[36] to obtain the full sensitivity enhancement available from echo train acquisition. It is important to note in Fig. 5(c) that with increasing ϵ_m, the lines of pure rotor-modulated evolution for both the even and odd echoes are not parallel to the lines of constant time. Thus, after the necessary affine transformation both even and odd signals will suffer from the same discontinuous T_2 dampening seen in the TOP-MAT experiment.

In the case of PASS, where modulated frequency evolution occurs in the indirect dimension, the train of echo-refocusing π pulses, shown as open rectangles in Fig. 5, must be shifted forward by ϵ_m. As shown in Fig. 5(b), the addition of the ϵ_m shift causes the rotor-modulated frequency evolution to refocus into an echo in the middle of each direct dimension of the echo train along the ϵ_u coordinate. Similarly, the ϵ_m shift leads to the unmodulated frequency evolution refocusing along the line $t^{(\mathrm{odd})} + \epsilon_u = 0$ in odd echoes and along the line $t^{(\mathrm{even})} - \epsilon_u = 0$ in even echoes of the train. Because of the delayed acquisition, the even PASS-ETA echoes are processed with the same affine transformation as the odd MAT-ETA echoes and the odd PASS-ETA echoes are processed with the same affine transformation as the even MAT-ETA echoes. Also note in Fig. 5(b) that with increasing ϵ_m the lines of pure rotor-modulated evolution in the odd echoes are parallel to the lines of constant time. Therefore, the signal from the odd echoes will not suffer from the discontinuous T_2 dampening artifact seen in the TOP-MAT experiment. For the even echoes, however, the lines of pure rotor-modulated evolution are not parallel to the lines of constant time. Thus, the even echoes suffer from the same discontinuous T_2 dampening seen in the TOP-MAT experiment. In fact, the lines of pure rotor-modulated evolution in the even echoes move away from the constant time line at twice the rate as the even and odd echoes in the MAT-ETA experiment. So, the even echoes in PASS-ETA will have stronger discontinuities in the T_2 dampening of its envelope along the pure unmodulated evolution dimension. In practice, since echo train acquisition is most advantageous when T_2 is long compared to the π pulse spacing, the discontinuous T_2 dampening artifact in even and odd MAT-ETA echoes and the even PASS-ETA echoes will likely be negligible. Of course, the odd-echo PASS-ETA will always be without such artifacts and can be readily used to verify the validity of the even-echo PASS-ETA signal.

1. TOP-MAT-PIETA and PASS-PIETA

One might think that the ETA approach of Carr-Purcell-Meiboom-Gill (CPMG)[37,38] can be easily appended to a sequence such as MAT or PASS to obtain enhanced sensitivity.[39] This approach, however, is not trivial for any phase modulated signal exiting the mixing period. Using CPMG on a phase modulated signal such as MAT or PASS would introduce a spectral artifact due to undesired coherence transfer pathways.[21,40–45] Traditional phase cycling[24,25] is out of the question for CPMG acquisition because the phase cycle for n refocusing pulses is, at minimum, 2^n steps. One simple solution for CPMG acquisition is to convert phase modulated coherence into amplitude modulation via a z-filter before conversion into observable coherence, but this comes with a loss in sensitivity. Gan and co-workers[20] showed that CPMG can be appended to MAT by employing a rather complicated phase cycle with multiplex acquisition scheme. Here we present a simpler alternative: Phase incremented echo train acquisition (PIETA).[21] In this approach the phase of every other refocusing pulse, ϕ, is incremented as a single variable, creating an additional phase dimension. The receiver phase is held constant in PIETA, avoiding cumbersome or intractable phase cycling schemes where the receiver phase must follow a master equation.[24,25] A Fourier transform with respect to the PIETA phase, ϕ, converts the ϕ dimension into a Δp dimension where desired signals are easily separated from undesired coherence transfer pathway signals. This is illustrated in Fig. 6 for the ^{29}Si TOP-MAT-PIETA experiment on a Cu(II)-doped mixed potassium/magnesium tetrasilicate glass. As acquired, this is a four-dimensional experiment, depending on ϵ_u, t, ϕ, and n (echo count). Figure 6 only shows a magnitude-mode cross section through the origin of ϵ_u and t. The general idea in PIETA is to collectively increment the phases of selected pulses so the desired pathway signals fall along the extremities of a sideways "V" pattern with undesired pathway signals appearing inside the sideways "V." In the case of TOP-MAT and PASS the π pulses in the preparation period are included in the PIETA phase increment so the desired signal in the first odd echo appears at $\Delta p = -6$ and desired signal in the first even echo the appears at $\Delta p = 6$. The positions of the desired signals in TOP-MAT-PIETA and TOP-PASS-PIETA as a function of echo count are given by

$$\Delta p(n) = (-1)^n \left\{ 2 \left\lfloor \frac{n-1}{2} \right\rfloor + 6 \right\}, \tag{13}$$

where $\lfloor x \rfloor$ represents the integer part or floor function of x. The desired even and odd echoes taken along Eq. (13) can be separated and both reduced down in a weighted average to maximize sensitivity[36] into even and odd 2D signals as a function of ϵ_u and t. The resulting signal can then be processed as one would have without PIETA. That is, even and odd 2D signals are each processed using the TOP approach as

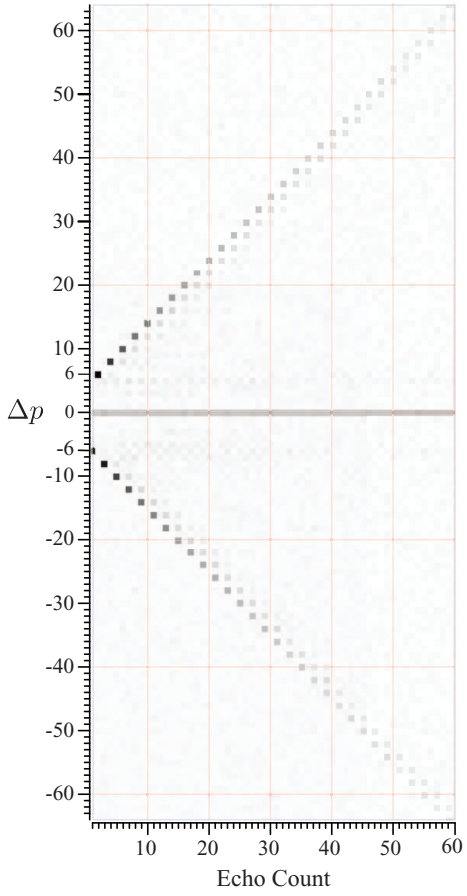

FIG. 6. Experimental 2D PIETA cross sections taken through the time origin of a ^{29}Si TOP-MAT-PIETA experiment on a Cu(II)-doped mixed potassium/magnesium tetrasilicate glass. The Δp range from -64 to $+64$ was obtained using $\Delta\phi_P = 2\pi/128$. Sixty PIETA echoes were acquired.

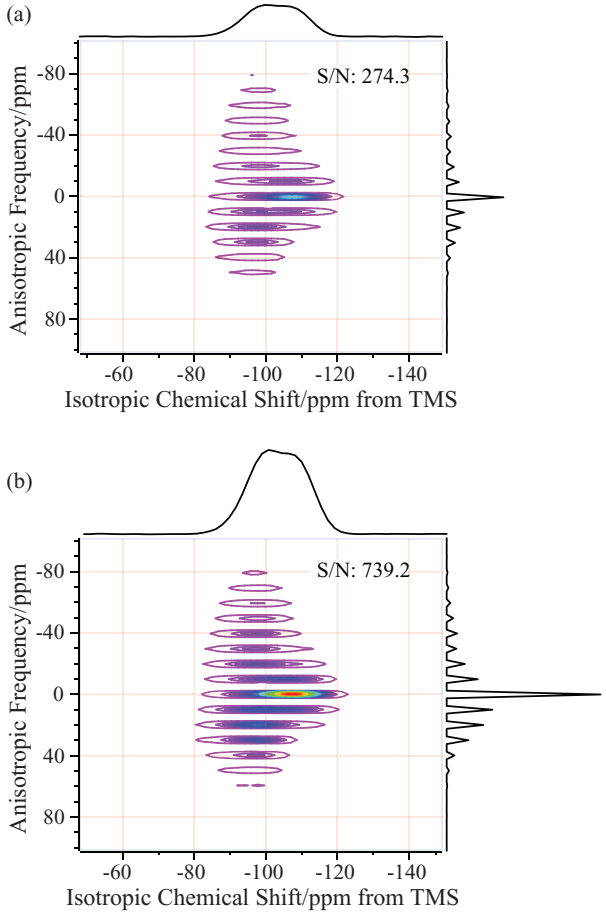

FIG. 7. Comparison of the TOP-MAT spectra of a Cu(II)-doped mixed potassium/magnesium tetrasilicate glass in which (a) a single shifted echo was acquired and (b) TOP-MAT-PIETA was used to acquire sixty echoes. All echoes were individually matched and coadded to produce the result. This procedure yields a MAT spectrum with a signal-to-noise ratio that is a factor 2.70 higher than the shifted echo experiment, with only a 1.5% increase of experiment time due to acquisition of multiple echoes.

described above, and finally combined into the final 2D TOP-MAT-PIETA spectrum correlating modulated and unmodulated evolution spectra shown in Fig. 7(b). For comparison, the 2D TOP-MAT of the same sample is shown in Fig. 7(a), demonstrating a PIETA sensitivity enhancement of 2.70.

In this tetrasilicate glass composition the ^{29}Si resonances arise from polymerized SiO_4 tetrahedra whose chemical shift anisotropy is related to the degree of connectivity of the tetrahedron to the network. Specifically, there are two types of environments in this glass composition: fully connected SiO_4 tetrahedra, $Q^{(4)}$ sites, having little to no anisotropy, and $Q^{(3)}$ sites, where only three oxygen are interconnecting, having a significant axially symmetric anisotropy.[46–49] From the changing width of the spinning sideband patterns in Fig. 7, it appears that the $Q^{(4)}$ sites fall in the region of isotropic chemical shifts from -120 ppm to -100 ppm while the $Q^{(3)}$ sites appear in the region from -100 ppm to -80 ppm. In a more detailed analysis of this ^{29}Si TOP-MAT-PIETA spectrum the statistical distribution of $Q^{(n)}$ can be determined. This spectrum along with ^{29}Si TOP-MAT-PIETA spectra of a series of other glasses with similar compositions will be analyzed and published elsewhere.

2. TOP-QMAT-PIETA and QPASS-PIETA

The ideas presented in this work can also be extended to the second-order broadened central transition of half-integer $I > \frac{1}{2}$ nuclei. When the electric quadrupole coupling of a nucleus is no longer negligible compared to the Zeeman coupling there will be second-order and possibly higher-order contributions to the NMR frequency. Using the notation of symmetry pathways,[9] the second-order contribution to NMR frequency is given by

$$\Omega_q^{(2)}(\Theta, m_i, m_j) = \frac{\omega_q^2}{\omega_0}[\mathbb{S}^{\{qq\}} \cdot \mathbb{c}_0(m_i, m_j)] + \frac{\omega_q^2}{\omega_0}[\mathbb{D}^{\{qq\}}(\Theta) \cdot \mathbb{c}_2(m_i, m_j)] + \frac{\omega_q^2}{\omega_0}[\mathbb{G}^{\{qq\}}(\Theta) \cdot \mathbb{c}_4(m_i, m_j)]. \quad (14)$$

Here $\mathbb{c}_0(m_i, m_j)$, $\mathbb{c}_2(m_i, m_j)$, and $\mathbb{c}_4(m_i, m_j)$ are spin transition symmetry functions, which are tabulated for various nuclear spin angular momenta, I, in Ref. 9, and $\mathbb{S}$, $\mathbb{D}(\Theta)$, and $\mathbb{G}(\Theta)$ represent the zero-, second-, and fourth-rank spa-

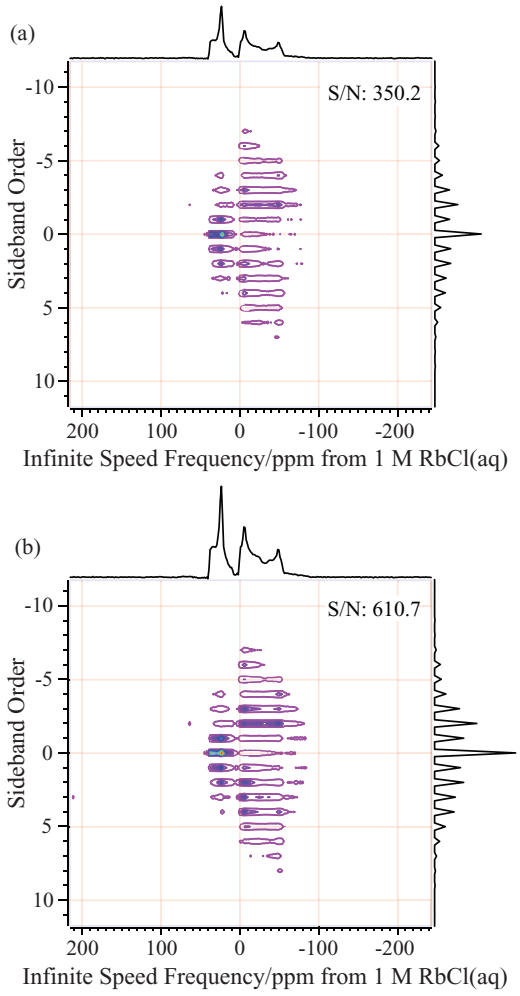

FIG. 8. Comparison of (a) shifted-echo TOP-QMAT and (b) TOP-QMAT-PIETA spectra of $^{87}Rb_2SO_4$. PIETA was used to acquire 22 echoes, which were individually matched and coadded to produce the result. This procedure yields a QMAT spectrum with a signal-to-noise ratio that is a factor of 1.74 greater than that of the shifted echo experiment, with a 15.7% increase in experiment time.

tial symmetry functions.[9] Additionally, Θ is the Euler angle specifying the orientation of sample in the laboratory frame, ω_0 is the Larmor frequency, and ω_q is the quadrupolar splitting given by

$$\omega_q = \frac{6\pi C_q}{2I(2I-1)}, \tag{15}$$

where C_q is the quadrupole coupling constant.

Under sample rotation one can show that Eq. (14) takes the form of Eq. (1) with values of $L = 0$, 2, and 4. With $L_{\max} = 4$, the MAT and PASS π timing solutions typically have nine π pulses.[50] Massiot *et al.*[23] introduced the QPASS experiment and Gan and co-workers[22] introduced the QMAT experiment for separating sidebands of the central transition of half-integer quadrupolar nuclei.

All the principles from this section can also be adapted in the design of the TOP-QMAT-PIETA and QPASS-PIETA experiments by simply using nine π pulses instead of five in the constant time preparation period of the sequence in Fig. 5(a). With the increase from five to nine π pulses, the positions of the desired signals in TOP-MAT-PIETA and TOP-PASS-PIETA as a function of echo count are given by

$$\Delta p(n) = (-1)^n \left\{ 2 \left\lfloor \frac{n-1}{2} \right\rfloor + 10 \right\}. \tag{16}$$

An experimental illustration of a ^{87}Rb TOP-QMAT-PIETA experiment on polycrystalline Rb_2SO_4 is shown in Fig. 8. Because MAS cannot fully average away the 4th-rank spatial anisotropy of second-order quadrupole broadening the projection on the unmodulated frequency dimension does not yield an isotropic spectrum. Instead, it only provides the infinite speed MAS spectrum. Since multiple sites have overlapping anisotropic resonances in the unmodulated frequency dimension the cross sections taken parallel to the modulated frequency (sideband order) dimension mix sideband contributions from overlapping resonances. Thus, the value of QMAT and QPASS is primarily in the projection onto the infinite speed dimension and the value of PIETA acquisition comes when transverse relaxation times are long enough to provide a significant sensitivity advantage. Clearly, the main application of QMAT or QPASS is eliminating spinning sidebands when the MAS speeds are insufficient. In such situations, however, the nutation frequency can be less than the anisotropic line width. Thus, resonance offset effects, which accumulate through the nine π pulses of QMAT or QPASS, can result in lineshape distortions in the "infinite speed" projection. Spectral intensities at larger resonance offsets can get reduced, although the positions of singularities in the powder pattern lineshape generally remain unchanged.

IV. SUMMARY

Multidimensional experiments for separating interactions are ubiquitous in NMR spectroscopy. While rotating samples create unique opportunities for separating anisotropic frequency contributions, the nonlinear equations that arise in this context can sometimes make understanding and designing experiments counterintuitive. We have attempted to present a simpler picture of how signal phase evolution arising from rotor modulated contributions to the NMR transition frequency can be separated from unmodulated contributions by viewing experiments, such as MAT and PASS, in coordinate systems that are related through affine transformations.

We have shown that a simple post-acquisition processing algorithm involving a double shear affine transformation, as used in processing signals from the TOP experiment,[16,31] can be used not only to reduce the number of measurements needed in the indirect dimension of the MAT experiment but can also eliminate truncated acquisition time artifacts. This solution, however, comes at the cost of introducing an artifact of discontinuous T_2 dampening of the MAT signal along the unmodulated evolution dimension. While TOP, PASS, and TOP-PASS avoid both of these artifacts, we found no solution for eliminating the discontinuous T_2 dampening artifact from MAT. Additionally, it is explained how to avoid introducing a third type of baseline signal artifact when applying the discrete Fourier transform to a 2D dimensional signal that

is periodic along the t_m coordinate, but aperiodic along the t_u coordinate.

In situations where there is an inhomogeneous distribution of unmodulated frequencies, as in the isotropic shifts of non-crystalline solids or the residual anisotropic shifts in the central transition of quadrupole nuclei, the addition of echo train acquisition to MAT or PASS can provide significant sensitivity gains. While the addition of echo train acquisition to MAT is relatively straightforward, the addition to PASS requires an understanding that the refocusing π pulses must be equally spaced and positioned at times where the total rotor modulated evolution phase is an integer multiple of 2π. Thus, echo train acquisition can be added to PASS simply by shifting the train of refocusing pulses by the indirect evolution time. Magic-Angle Turning with echo train acquisition still remains tainted by discontinuous T_2 dampening along the unmodulated evolution dimension. While the T_2 dampening of unmodulated evolution dimension in the odd echoes of PASS remains continuous, the even echoes of PASS suffer from the same discontinuous T_2 dampening seen in the MAT experiment.

Generally, echo train acquisition cannot be added to NMR pulse sequences with a phase modulated signal exiting the mixing period, such as MAT or PASS, without taking special precautions to prevent artifact signals from undesired coherence transfer pathways from contaminating the signal. We have showed how PIETA provides a robust implementation of echo train acquisition for MAT and PASS, eliminating artifacts without the time consuming constraints of traditional phase cycling schemes at a minor cost of additional post-acquisition signal processing. Combining these ideas together we demonstrate enhanced sensitivity with a TOP-MAT-PIETA sequence on ^{29}Si NMR of a silicate glass where different silicate tetrahedra environments can be distinguished by distinctly different spinning sideband patterns. Likewise, we adapt these approaches in the TOP-QMAT-PIETA experiment, which provides an "infinite speed" MAS spectrum of the central transition of half-integer quadrupolar nuclei, to provide enhanced sensitivity.

Phase incremented echo train acquisition, unlike CPMG, provides the opportunity to turn echo train acquisition into a *J*-resolved dimension[21] and future work along these lines is in progress. Finally, although these ideas were initially developed in the field solid-state NMR they are also applicable in the realm of magnetic resonance imaging of rotating samples[3,4] including recent work by Sakellariou and coworkers.[5]

ACKNOWLEDGMENTS

This material is based upon work supported by the National Science Foundation under Grant No. NSF CHE-1012175. The authors would like to thank Eric Keeler for synthesis of the $KMg_{0.5}O \cdot 4SiO_2$ glass, and Michael Davis for helpful discussions during the early stages of this work.

[1] G. A. Williams and H. S. Gutowsky, Phys. Rev. **104**, 278 (1956).
[2] M. M. Maricq and J. S. Waugh, J. Chem. Phys. **70**, 3300 (1979).
[3] Y. Ogura and K. Sekihara, J. Magn. Reson. **92**, 490 (1991).
[4] J. H. Baltisberger, S. Hediger, and L. Emsley, J. Magn. Reson. **172**, 79 (2005).
[5] A. Wong and D. Sakellariou, Chem. Phys. Chem. **12**, 3529 (2011).
[6] W. T. Dixon, J. Chem. Phys. **77**, 1800 (1982).
[7] N. M. Szeverenyi, A. Bax, and G. E. Maciel, J. Magn. Reson. **61**, 441 (1985).
[8] A. Samoson, B. Q. Sun, and A. Pines, "New angles in motional averaging," in *Pulsed Magnetic Resonance: NMR, ESR, and Optics – A Recognition of E. L. Hahn* (Clarendon Press, Oxford, 1992), pp. 80–94.
[9] P. J. Grandinetti, J. T. Ash, and N. M. Trease, Prog. Nucl. Magn. Reson. Spectrosc. **59**, 121 (2011).
[10] Z. H. Gan, J. Am. Chem. Soc. **114**, 8307 (1992).
[11] J. Z. Hu, D. W. Alderman, C. H. Ye, R. J. Pugmire, and D. M. Grant, J. Magn. Reson. A **105**, 82 (1993).
[12] S. L. Gann, J. H. Baltisberger, and A. Pines, Chem. Phys. Lett. **210**, 405 (1993).
[13] O. N. Antzutkin, S. C. Shekar, and M. H. Levitt, J. Magn. Reson. A **115**, 7 (1995).
[14] O. N. Antzutkin, Prog. Nucl. Magn. Reson. Spectrosc. **35**, 203 (1999).
[15] D. W. Alderman, G. McGeorge, J. Z. Hu, R. J. Pugmire, and D. M. Grant, Mol. Phys. **95**, 1113 (1998).
[16] M. Davis, K. M. Shookman, J. D. Sillaman, and P. J. Grandinetti, J. Magn. Reson. **210**, 51 (2011).
[17] B. Blümich, P. Blumler, and J. Jansen, Solid State Nucl. Magn. Reson. **1**, 111 (1992).
[18] P. Blumler, B. Blümich, and J. Jansen, Solid State Nucl. Magn. Reson. **3**, 237 (1994).
[19] I. Hung and Z. H. Gan, J. Magn. Reson. **204**, 150 (2010).
[20] I. Hung, T. Edwards, S. Sen, and Z. H. Gan, J. Magn. Reson. **221**, 103 (2012).
[21] J. H. Baltisberger, B. J. Walder, E. G. Keeler, D. C. Kaseman, K. J. Sanders, and P. J. Grandinetti, J. Chem. Phys. **136**, 211104 (2012).
[22] I. Hung and Z. H. Gan, Chem. Phys. Lett. **496**, 162 (2010).
[23] D. Massiot, V. Montouillout, F. Fayon, P. Florian, and C. Bessada, Chem. Phys. Lett. **272**, 295 (1997).
[24] G. Bodenhausen, H. Kogler, and R. R. Ernst, J. Magn. Reson. **58**, 370 (1984).
[25] A. D. Bain, J. Magn. Reson. **56**, 418 (1984).
[26] P. J. Grandinetti, J. H. Baltisberger, A. Llor, Y. K. Lee, U. Werner, M. A. Eastman, and A. Pines, J. Magn. Reson. A **103**, 72 (1993).
[27] F. Fayon, C. Bessada, A. Douy, and D. Massiot, J. Magn. Reson. **137**, 116 (1999).
[28] F. G. Vogt, J. M. Gibson, D. J. Aurentz, K. T. Mueller, and A. J. Benesi, J. Magn. Reson. **143**, 153 (2000).
[29] R. N. Bracewell, K.-Y. Chang, A. K. Jha, and Y.-H. Wang, Electron. Lett. **29**, 304 (1993).
[30] G. Otting, H. Widmer, G. Wagner, and K. Wüthrich, J. Magn. Reson. **66**, 187 (1986).
[31] D. Massiot, J. Hiet, N. Pellerin, F. Fayon, M. Deschamps, S. Steuernagel, and P. J. Grandinetti, J. Magn. Reson. **181**, 310 (2006).
[32] While the TOP shear factors given here are the same as those given by Davis *et al.*,[16] the scaling factor given by Davis *et al.*[16] was incorrect.
[33] M. Strohmeier, D. W. Alderman, and D. M. Grant, J. Magn. Reson. **155**, 263 (2002).
[34] M. Eden and M. H. Levitt, J. Magn. Reson. **132**, 220 (1998).
[35] W. H. Press, S. A. Teukolsky, W. T. Vetterling, and B. P. Flannery, *Numerical Recipes* (Cambridge University Press, New York, NY, 1992).
[36] K. Dey, J. T. Ash, N. M. Trease, and P. J. Grandinetti, J. Chem. Phys. **133**, 054501 (2010).
[37] H. Y. Carr and E. M. Purcell, Phys. Rev. **94**, 630 (1954).
[38] S. Meiboom and D. Gill, Rev. Sci. Instrum **29**, 688 (1958).
[39] D. Sakellariou and T. Charpentier, Appl. Magn. Reson. **32**, 583 (2007).
[40] R. L. Vold, R. R. Vold, and H. E. Simon, J. Magn. Reson. **11**, 283 (1973).
[41] G. Gaelman and M. G. Prammer, J. Magn. Reson. **113**, 11 (1995).
[42] J. Simbrunner and R. Stollberger, J. Magn. Reson. B **109**, 301 (1995).
[43] A. Ross, M. Czisch, and G. C. King, J. Magn. Reson. **124**, 355 (1997).
[44] F. Bălibanu, K. Hailu, R. Eymael, D. Demco, and B. Blümich, J. Magn. Reson. **145**, 246 (2000).
[45] Y.-Q. Song, J. Magn. Reson. **157**, 82 (2002).

[46]P. Zhang, C. Dunlap, P. Florian, P. J. Grandinetti, I. Farnan, and J. F. Stebbins, J. Non.-Cryst. Solids **204**, 294 (1996).
[47]P. Zhang, P. J. Grandinetti, and J. F. Stebbins, J. Phys. Chem. B **101**, 4004 (1997).
[48]M. Davis, D. C. Kaseman, S. M. Parvani, K. J. Sanders, P. J. Grandinetti, P. Florian, and D. Massiot, J. Phys. Chem. A **114**, 5503 (2010).
[49]M. Davis, K. J. Sanders, P. J. Grandinetti, S. J. Gaudio, and S. Sen, J. Non.-Cryst. Solids **357**, 2787 (2011).
[50]W. T. Dixon, J. Magn. Reson. **64**, 332 (1985).
[51]See supplementary material at http://dx.doi.org/10.1063/1.4803142 for a derivations of MAT and PASS timing solutions, and for further details on the shifted-echo MAT and PASS pulse sequence.

Supporting Information: Sideband Separation Experiments in NMR with Phase Incremented Echo Train Acquisition

Brennan J. Walder,[1] Krishna K. Dey,[2] Derrick C. Kaseman,[1] Jay H. Baltisberger,[3] and Philip J. Grandinetti[1, a)]
[1)] *Department of Chemistry, Ohio State University, 100 West 18th Avenue, Columbus, OH 43210, USA*
[2)] *Center of Biomedical Magnetic Resonance, SGPGIMS campus, Lucknow, India*
[3)] *Division of Natural Science, Mathematics, and Nursing, Berea College, Berea, Kentucky 40403*

(Dated: 3 July 2013)

I. MAT AND PASS TIMING SOLUTIONS

The NMR signal in a rotating sample can be manipulated into a number of desirable forms by applying a series of π pulses between the initial excitation pulse and the start of signal acquisition. In the PASS and MAT experiments[1,2], a time coordinate is defined where the initial excitation pulse is applied at $t = -T$ and signal acquisition begins at $t = 0$. Between the initial excitation pulse and signal acquisition are Q π-pulses, applied at times $-T+\tau_1, -T+\tau_2, \ldots, -T+\tau_Q$. The signal phase at $t = 0$, a duration of $\tau_{Q+1} = T$ after the initial excitation pulse, is given by

$$\begin{aligned}\Phi_Q(t=0) &= (-1)^Q \sum_{q=0}^{Q} (-1)^q \int_{-T+\tau_q}^{-T+\tau_{q+1}} \Omega(t')dt', \\ &= W_0 \left[T - 2(-1)^Q \sum_{q=1}^{Q} (-1)^q \tau_q \right] \\ &+ \sum_{l=1}^{L_{\max}} \sum_{\substack{k=-l \\ k\neq 0}}^{l} W_{l,k}(\chi_R) \\ &\times \left[1 - 2(-1)^Q \sum_{q=1}^{Q} (-1)^q e^{ik\theta_q} e^{-ik\theta_T} - (-1)^Q e^{-ik\theta_T} \right], \end{aligned} \tag{1}$$

where $\tau_0 = 0$, $\theta_T = \omega_R T$, $\theta_q = \omega_R \tau_q$, and $L_{\max}$ is the rank of the highest spatial tensor contributing to the NMR transition frequency. We constrain the initial rotor phase, χ_R, to be identical in every PASS or MAT experiment. In polycrystalline samples, however, this constraint is unnecessary[3].

A. PASS

In the PASS experiment[1,4] the timings of the Q π pulses are manipulated so the signal phase at $t = 0$ has a form

$$\Phi_{\text{PASS}}(\epsilon_m, t=0) = W_0 \cdot [\ 0\ ] - \sum_{l=1}^{L_{\max}} \sum_{\substack{k=-l \\ k\neq 0}}^{l} W_{l,k}(\chi_R) \left[e^{ik\omega_R \epsilon_m} - 1 \right], \tag{2}$$

where ϵ_m is a function of the Q π pulse timings. Evolving forward from $t = 0$ the PASS signal phase then becomes similar to the Bloch decay MAS signal

$$\Phi_{\text{PASS}}(\epsilon_m, t) = W_0\ t + \sum_{l=1}^{L_{\max}} \sum_{\substack{k=-l \\ k\neq 0}}^{l} W_{l,k}(\chi_R) \left[e^{ik\omega_R t} - e^{ik\omega_R \epsilon_m} \right], \tag{3}$$

with the important exception that ϵ_m is non-zero and can be varied independent of t. From the last term in square brackets in Eq. (3) it is clear that the modulated frequency contribution refocuses during t when $t - \epsilon_m = 0$.

The π pulse timings for the PASS experiment come from equating Eqs. (1) and (2) to obtain the Dixon equations:

$$\theta_T - 2(-1)^Q \sum_{q=1}^{Q} (-1)^q \theta_q = 0, \tag{4}$$

and

$$e^{ik\Theta_m} = 2(-1)^Q \sum_{q=1}^{Q} (-1)^q e^{ik\theta_q} e^{-ik\theta_T} + (-1)^Q e^{-ik\theta_T}, \tag{5}$$

where $\Theta_m = \omega_R \epsilon_m$. Levitt and coworkers[2] suggested a 2D PASS experiment of constant duration T with $\theta_T = 2\pi$ and for odd values of Q obtained the equations

$$2 \sum_{q=1}^{Q} (-1)^q \theta_q + 2\pi = 0, \tag{6}$$

and

$$-2 \sum_{q=1}^{Q} (-1)^q e^{ik\theta_q} - 1 = e^{ik\Theta_m}, \quad \text{for } k = 1, \ldots, L_{\max}. \tag{7}$$

These equations can be solved numerically in the case where $L_{\max} = 2$ for the five π pulse timings shown in Fig. 1 and tabulated elsewhere[2].

[a)] http://www.grandinetti.org

B. MAT

In the MAT experiment the timings of the Q π pulses are manipulated so the signal phase at $t = 0$ has a form

$$\Phi_{\mathrm{MAT}}(\epsilon_u, t = 0) = -W_0\epsilon_u, \tag{8}$$

where ϵ_u is a function of the Q π pulse timings.

Evolving forward from $t = 0$ the MAT signal phase then becomes similar to the Bloch decay MAS signal

$$\Phi_{\mathrm{MAT}}(\epsilon_u, t) = W_0\ (t - \epsilon_u) + \sum_{l=1}^{L_{\max}} \sum_{\substack{k=-l \\ k\neq 0}}^{l} W_{l,k}(\chi_R)\left[e^{ik\omega_R t} - 1\right], \tag{9}$$

with the important exception that ϵ_u is non-zero and can be varied independent of t. From the last term in square brackets in Eq. (9) it is clear that the unmodulated frequency contribution refocuses during t when $t-\epsilon_u = 0$.

The π pulse timings for the MAT experiment come from equating Eqs. (1) and (8) to obtain the equations:

$$-\theta_T + 2(-1)^Q \sum_{q=1}^{Q}(-1)^q\theta_q = \Theta_u, \tag{10}$$

and

$$2(-1)^Q \sum_{q=1}^{Q}(-1)^q e^{ik\theta_q}e^{-ik\theta_T} + (-1)^Q e^{-ik\theta_T} = 1, \tag{11}$$

where $\Theta_u = \omega_R\epsilon_u$. A 2D MAT experiment, of constant duration T with $\theta_T = 2\pi$ and odd values of Q, leads to the equations

$$-2\sum_{q=1}^{Q}(-1)^q\theta_q - 2\pi = \Theta_u, \tag{12}$$

and

$$\sum_{q=1}^{Q}(-1)^q e^{ik\theta_q} + 1 = 0, \quad \text{for } k = 1, \ldots, L_{\max}. \tag{13}$$

Analytic solutions for this problem can be derived based upon symmetry arguments[5]. A solution with $Q = 2L_{\max} + 1$ is given by

$$\theta_q = \frac{\pi}{L_{\max} + 1}\left[q + \left[1 - (-1)^q\right]\frac{\Theta_u}{4\pi}\right]. \tag{14}$$

In this solution the π pulses associated with even q are stationary in time and equally spaced at integer multiples of $t_R/(L_{\max} + 1)$, whereas the π pulses associated with odd q have timings that increase linearly with ϵ_u and occur precisely at the midpoint of the interval between neighboring even q pulses when $\epsilon_u = 0$.

[1] W. T. Dixon, J. Chem. Phys. **77**, 1800 (1982).
[2] O. N. Antzutkin, S. C. Shekar, and M. H. Levitt, J. Magn. Reson. A **115**, 7 (1995).
[3] M. H. Levitt, J. Magn. Reson. **82**, 427 (1989).
[4] W. T. Dixon, J. Magn. Reson. **44**, 220 (1981).
[5] O. N. Antzutkin, Prog. NMR Spect. **35**, 203 (1999).
[6] J. H. Baltisberger, B. J. Walder, E. G. Keeler, D. C. Kaseman, K. J. Sanders, and P. J. Grandinetti, J. Chem. Phys. **136**, 211104 (2012).

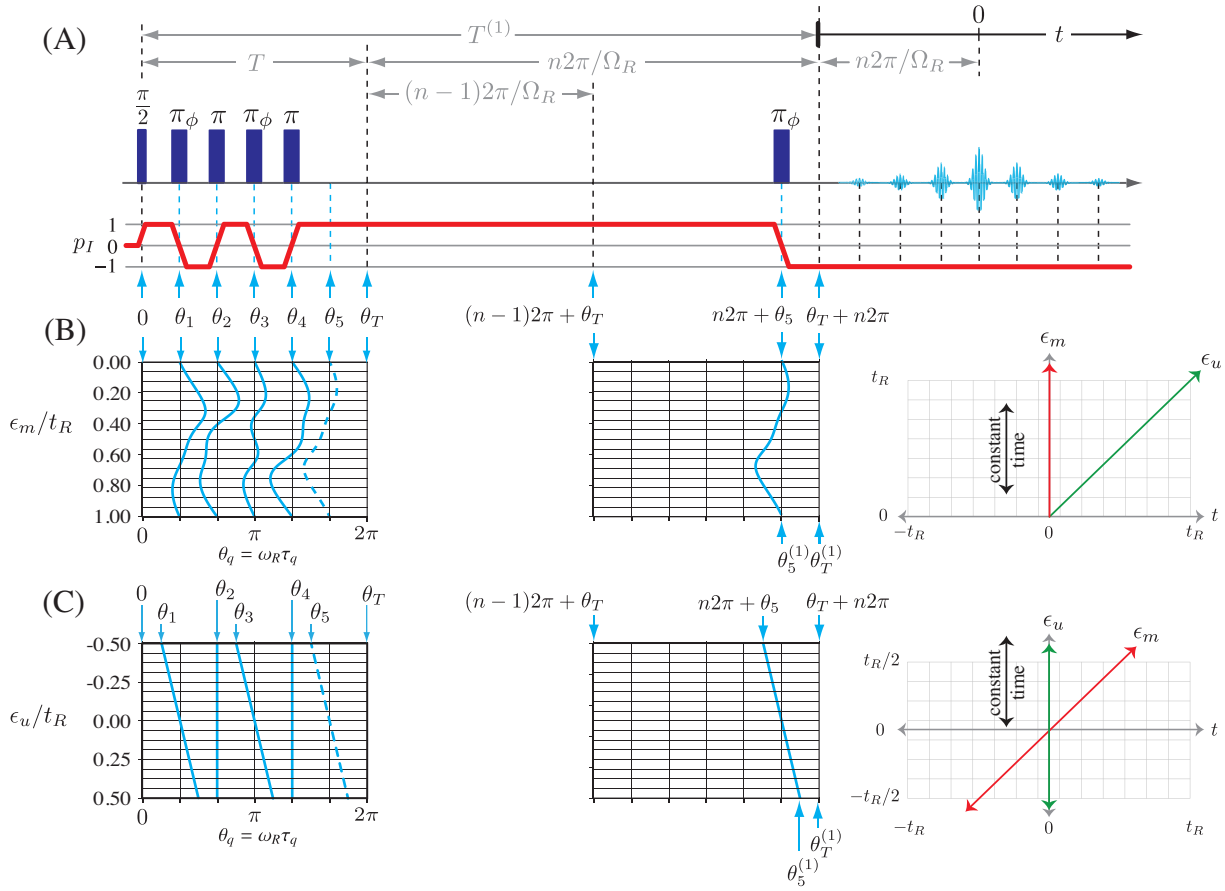

FIG. 1. (A) A generic five π pulse shifted-echo sequence $L_{\max}=2$ for PASS and MAT along with p_I symmetry pathway for samples with second-rank anisotropies. The θ_j values represent the rotor position $\theta_j=\omega_R t_j$ where t_j is the time from the initial excitation pulse. Instead of traditional phase cycling, the signal is acquired with a constant receiver phase while the phase of all π pulses with the ϕ subscript are incremented together into a single phase dimension[6]. (B) The π pulse timings for the PASS experiment and the lines in the ϵ_m–t coordinates where the unmodulated and modulated evolutions refocus into echoes. Below are the relevant effective symmetry pathways. (C) The π pulse timings for the MAT experiment and the lines in the ϵ_u–t coordinates where the unmodulated and modulated evolutions refocus into echoes. In both (B) and (C) the direction of constant time relative to the initial excitation pulse is indicated.